Miniature tapered photonic crystal fiber interferometer with enhanced sensitivity by acid microdroplets etching

Sun-jie Qiu, Ye Chen, Jun-long Kou, Fei Xu,* and Yan-qing Lu

College of Engineering and Applied Sciences and National Laboratory of Solid State Microstructures, Nanjing University, Nanjing 210093, China

*Corresponding author: feixu@nju.edu.cn

Received 29 March 2011; accepted 12 June 2011;
posted 20 June 2011 (Doc. ID 144882); published 22 July 2011

We fabricate a miniature tapered photonic crystal fiber (PCF) interferometer with enhanced sensitivity by acid microdroplets etching. This method is very simple and cost effective, avoiding elongating the PCF, moving and refixing the device during etching, and measuring. The refractive index sensing properties with different PCF diameters are investigated both theoretically and experimentally. The tapering velocity can be controlled by the microdroplet size and position. The sensitivity greatly increases (five times, 750 nm/RIU) and the size decreases after slightly tapering the PCF. The device keeps low temperature dependence before and after tapering. More uniformly and thinly tapered PCFs can be realized with higher sensitivity (~100 times) by optimizing the etching process.

OCIS codes: 060.5295, 060.2370, 120.3180, 280.4788.

1. Introduction

Fiber in-line modal interferometers based on photonic crystal fibers (PCFs), also known as microstructured optical fibers, can be fabricated in a number of ways, and their properties and applications have been widely studied. [1–6] Different types of PCF modal interferometers are mostly used in applications such as strain and temperature sensing. [4,7] Refractive index sensing for biological and chemical applications can also be realized by PCF interferometers, but, in most of these techniques, the samples have to be infiltrated into the holes of the PCF, the PCF is tens of centimeters long, and the response rate is poor. A compact PCF interferometer built via fusing splicing was reported and attracted a lot of interest. This kind of device consists of a stub of 125 um large-mode-area (LMA) PCF spliced between the same size standard single-mode fibers (SMFs). In the spliced regions, the voids of the PCF fully collapsed, thus allowing the coupling and recombination of PCF core and cladding modes, and the cladding mode is sensitive to outside environment, so it is suitable for measuring indices through interaction of the evanescent field and the analyte in the outer region of the PCF section. The fabrication of the device is very simple, only involving cleaving and splicing processes that can be carried out in a standard fiber optics lab. [8,9] The device is cost effective, highly stable over time, has low temperature sensitivity, and only needs a small piece of cheap commercial LMA PCF in the standard size (~2 cm long, 125 um in diameter). [8,9] However, this kind of sensor also suffers from low sensitivity because of the limited evanescent field by the large fiber size. Tapering PCF is a possible solution to enhance the available evanescent field and increase the sensitivity, but one major drawback is that it will extend the size a lot. Another problem is that it is challenging to taper such a small piece of PCF and prevent the holes from collapsing and keep the interference properties by the conventional "slow-and-hot" method. [10].

In this paper, we fabricated a miniature tapered PCF interferometer with enhanced sensitivity by a

0003-6935/11/224328-05$15.00/0

new acid-etching method with acid microdroplets. [11] This method is very simple and cost effective, without elongating the PCF and moving and refixing the device during etching and sensitivity measuring. The refractive index sensing properties with different PCF diameters are investigated both theoretically and experimentally. The tapering velocity can be controlled by the microdroplet size and position. The refractive index sensitivity greatly increases (five times), and the size decreases after tapering the PCF, while the temperature sensitivity does not change a lot, keeping low temperature dependence for both the tapered and untapered PCF interferometers. The total sensor size is only several millimeters long and tens of micrometers thick. [8,9] The sensitivity of 750 nm/RIU (refractive index unit) is also much higher than recent results utilizing the same mechanism. [8,9] More uniformly and thinly tapered PCFs can be realized with higher sensitivity (~100 times) by optimizing the etching process.

2. Fabrication Method of Tapered PCF Interferometer Sensors

For the construction of the tapered PCF interferometer, we employed a commercial single-mode PCF (LMA-8, NKT Photonics) consisting of a solid core surrounded by six rings of air holes. As shown in Fig. 1(a), such a fiber has an 8.4 μm diameter core, voids with an average diameter of 2.17 μm, and the average separation between the voids is 5.3 μm. The diameter of the PCF is the same as SMF-28 fibers and it is cheaper and easier to be spliced to SMF-28 with higher stability and better repetition, compared with other larger-sized PCFs. Initially, a PCF interferometer was fabricated by splicing the ends of two SMF-28 fibers to the cleaved end of a few millimeters of PCF. The voids of the PCF collapsed completely over a short region about several hundred micrometers long. Then, this device was tapered by a simple hydrofluoric acid (HF) microdroplet etching method. [11] The device was held by two clamps across an HF-resistant dish. We then dropped an acid microdroplet with 40% HF onto the dish. The dish could be raised by a translation stage to immerse the fiber in the droplet to initiate etching. The droplet shape allowed the length of the waist region to be controlled by the immersion depth. The apparatus was situated on an optical table for mechanical stability, and the experiments were performed at room temperature. The tapered PCF was monitored with a microscope *in situ* and in real time during etching. In general, the tapered PCF is more uniform and the average diameter is smaller if it is etched with a larger acid microdroplet. For the thinnest waist of the tapered PCF, the etching velocity is ~2 μm/ min. Figure 1(c) shows the pictures before etching and after 29 min of etching. The diameter is about 68 μm at $t = 29$ min.

In fact, this setup was also used for sensing measurement in our experiment. Instead of the large acid baths in traditional etch techniques, our setup avoids moving the PCF piece and refixing the fibers during tapering and sensing measurement, which is very important and useful because the optical modes in the PCF piece of this device are very sensitive to bending and twisting. Compared with the slow-and-hot or heat-and-pull technique, [12–14] this method is much simpler and, more importantly, the PCF will not be elongated.

3. Theory and Simulation

When the light travels from the SMF to the tapered PCF [Fig. 1(b)] in the interferometer, the SMF fundamental mode begins to diffract. When it enters the collapsed PCF region, it excites core and cladding modes in the PCF section with different propagation constants [4,8,9]. After propagating in the PCF, the modes reach the other collapsed end of the PCF. They will thus further diffract and will be recombined through the filtering of the subsequent SMF. Therefore, the transmission of our interferometer can be expressed as that of a two-mode interferometer [8]:

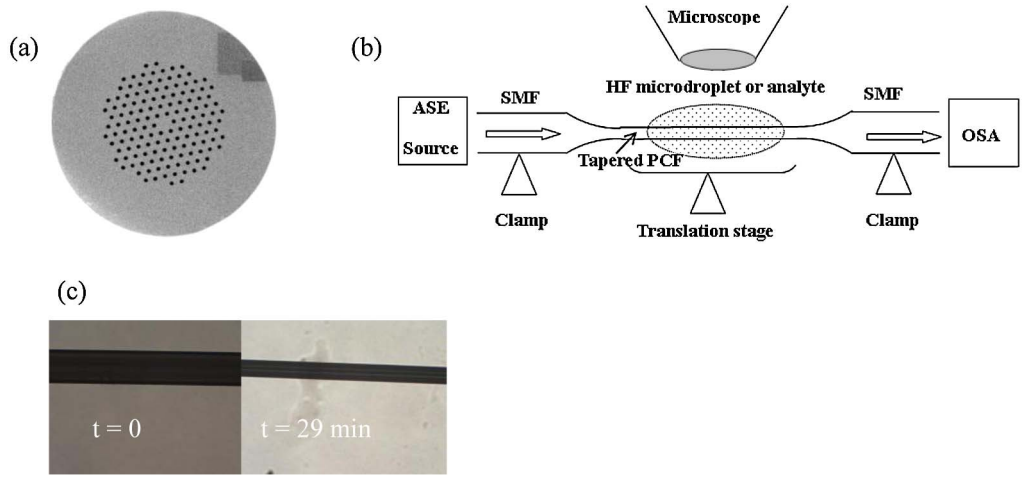

Fig. 1. (Color online) (a) Scanning electron microscope image of the cross section of the PCF used for the experiment. (b) Schematic of the experimental setup for tapering and sensing measurement. The PCF length is L and the diameter of the tapered PCF is D. OSA, optical spectrum analyzer. (c) Pictures of the PCF before etching and after 29 min of etching.

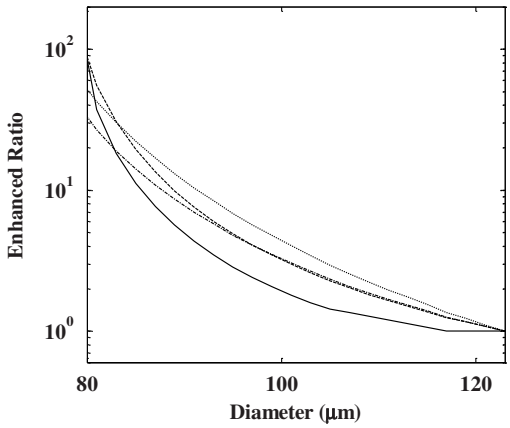

Fig. 2. Enhanced ratios for several cladding modes as a function of the diameter of a tapered PCF.

$$I = I_{co} + I_{cl} + 2\sqrt{I_{co}I_{cl}}\cos(\delta + \varphi_0), \quad (1)$$

$$\text{Free spectral range (FSR)} = 2\pi\lambda/\delta, \quad (2)$$

where $\delta = (2\pi/\lambda)\int_L (n_{cl} - n_{co})dz$, I is the intensity of the interference signal, and I_{co} and I_{cl} are the intensities of the core and cladding modes. δ is the phase difference of the two modes; n_{co} and n_{cl} are the effective indices of the core and cladding modes, which depend on the local diameter D of the tapered PCF if the taper is not uniform. λ is the wavelength.

If the tapered PCF is surrounded by a certain analyte (n_a), n_{cl} changes with n_a because of the interaction between the analyte and evanescent field of the cladding mode. When D is large, n_{co} is constant because the core mode is isolated from the outside environment. The refractive index sensitivity S is defined as the interference wavelength (λ_i) shift divided by the corresponding n_a change:

$$S = \frac{d\lambda_i}{dn_a} = \frac{\lambda_i}{n_{cl} - n_{co}} \frac{\partial(n_{cl} - n_{co})}{\partial n_a}. \quad (3)$$

In order to compare the sensitivities at different diameters, we define the enhanced ratio as the ratio of the sensitivity from $D < 125\,\mu$m (tapered) to $D = 125\,\mu$m (untapered). The enhanced ratio depends on both the diameter and the excited cladding modes.

Figure 2 shows the enhanced ratios for several typical cladding modes at $n_a = 1.37$. The sensitivities for different modes have a similar trend and increase with the decreasing diameter very quickly, as we expected. It can increase nearly 100 times at $D = 80$ μm. In our simulation, we only consider the case of slightly etched PCF ($D > 80\,\mu$m), which means that only the solid cladding becomes thin but the core and the air rings keep the original shapes.

4. Experimental Results

In order to detect the interferometric behavior of the tapered PCF interferometers, a broadband amplified spontaneous emission source and an optical spectrum analyzer were employed during the whole experiment in real time as shown in Fig. 1(b). A piece of PCF with a length of ~11 mm was spliced to SMFs, and then we etched this PCF and measured the spectra alternately. Every time after tapering and before measuring the spectra, the HF droplet was removed and the PCF was cleaned and dried in air. Then the interference spectra were measured in air, acetone, isopropanol, mixtures of isopropanol, and acetone, respectively. The aqueous solutions were added on a dish and the dish was raised by a translation stage to immerse the fiber. In our experiment, the tapered PCF interferometer did not need to be moved and refixed, which was important to avoid the influence of bending and twisting. All these tapered PCF interferometers were formed from and compared with the same originally untapered PCF interferometer. The refractive indices of pure isopropanol and acetone at 1.55 μm are 1.3739 and 1.3577, respectively. [15].

In our experiment, we slightly etched two untapered PCF interferometers ($L \sim 11$ mm) for refractive index and temperature measurement, respectively. Figure 3(a) shows the measured interference spectra of a PCF interferometer in air before and after the

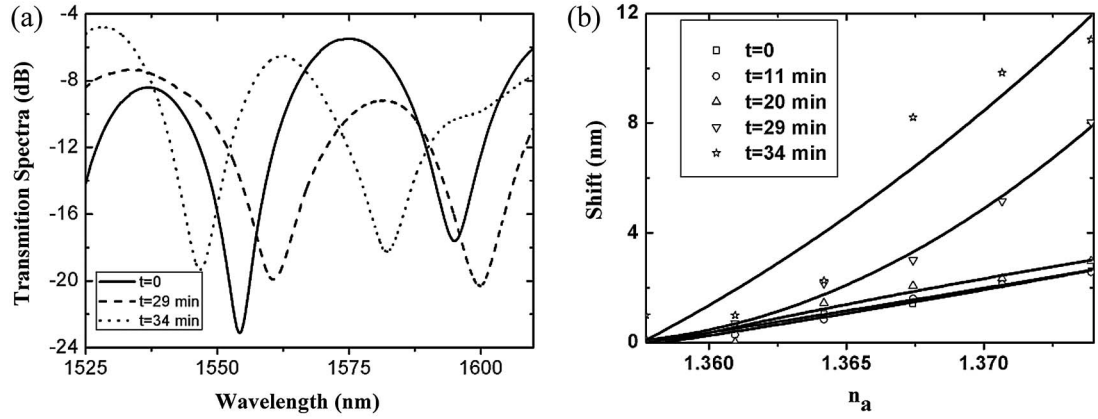

Fig. 3. (a) Interference spectra of the tapered PCF interferometers in air. (b) Wavelength shifts due to surrounding refractive index changes before and after the interferometer was etched by a small HF microdroplet. Here, the etching time t is the total time accumulated by all these tapering periods before the spectra were measured.

Table 1. Sensitivity at Different Etching Times

t (min)	0	11	20	29	34
Sensitivity (nm/RIU)	152	162	193	500	750

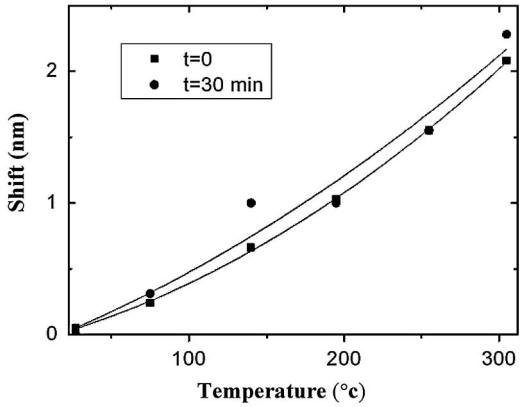

Fig. 4. Wavelength shifts due to temperature change before and after the interferometer was etched by HF microdroplets.

interferometer was etched. Here, the etching time t is the total time accumulated by all these tapering periods before the spectra were measured. The FSR is large (~40 nm) because of the ultrashort PCF; it is also close to the theoretical result [~48 nm from Eq. (2)]. Figure 3(b) shows that the wavelength shifts due to the surrounding refractive index changed in the mixtures of acetone and isopropanol before and after this interferometer was etched. As shown in Table 1, the sensitivity at $t = 0$ (untapered PCF interferometer) is ~150 nm/RIU and increases with more etching time (smaller averaged taper diameter), and it can be as high as 750 nm/RIU at $t = 34$ min, five times as high as $t = 0$ and much higher than previous results of this kind of PCF interferometer. The thinner waist of the tapered PCF is ~60 μm at $t = 34$ min and several air holes at the edge of air rings were etched at such a size. The enhanced ratio is similar with the calculated one at a D of 80–90 μm. It is reasonable if the tapered PCF is not uniform, the thinnest waist is very short and the averaged diameter of the nonuniformly tapered PCF is about 80 μm. If we can optimize the etching process in the future, more uniformly tapered PCFs can be realized with higher sensitivity.

We etched another untapered PCF interferometer ($L \sim 11$ mm) and compared the temperature sensitivities. Figure 4 shows the wavelength shifts due to temperature change before and after the interferometer was etched. The temperature sensitivity does not change a lot and it keeps low temperature dependence for both the tapered and untapered PCF interferometers.

5. Summary

We fabricated a miniature tapered PCF interferometer with enhanced sensitivity by acid microdroplets. This method is very simple and cost effective, avoiding elongating the PCF, moving and refixing the device during etching, and measuring the sensitivity. The refractive index sensing properties with different PCF diameters are investigated both theoretically and experimentally. The tapering velocity can be controlled by the microdroplet size and position. The sensitivity greatly increases (five times, 750 nm/RIU) and the size decreases after tapering the PCF. Smaller size and higher sensitivity (~100 times larger than an untapered device) can be realized with more uniformly tapered PCFs by optimizing the etching process. Moreover, the temperature sensitivity does not change a lot and keeps low temperature dependence for both the tapered and untapered PCF interferometers.

This work is supported by the National 973 program under contracts 2010CB327800 and 2011CBA00200 and the National Natural Science Foundation of China (NSFC) programs 11074117 and 60977039. The authors also acknowledge support from the New Century Excellent Talents program and the Changjiang Scholars program.

References

1. J. Ju, Z. Wang, W. Jin, and M. S. Demokan, "Temperature sensitivity of a two-mode photonic crystal fiber interferometric sensor," IEEE Photon. Technol. Lett. **18**, 2168–2170 (2006).
2. O. Frazao, J. L. Santos, F. M. Araujo, and L. A. Ferreira, "Optical sensing with photonic crystal fibers," Laser Photon. Rev. **2**, 449–459 (2008).
3. X. Y. Dong, H. Y. Tam, and P. Shum, "Temperature-insensitive strain sensor with polarization-maintaining photonic crystal fiber based Sagnac interferometer," Appl. Phys. Lett. **90**, 151113 (2007).
4. J. Villatoro, V. Finazzi, V. P. Minkovich, V. Pruneri, and G. Badenes, "Temperature-insensitive photonic crystal fiber interferometer for absolute strain sensing," Appl. Phys. Lett. **91**, 091109 (2007).
5. J. Villatoro, M. P. Kreuzer, R. Jha, V. P. Minkovich, V. Finazzi, G. Badenes, and V. Pruneri, "Photonic crystal fiber interferometer for chemical vapor detection with high sensitivity," Opt. Express **17**, 1447–1453 (2009).
6. S. Y. Zhang, Q. Zhong, X. S. Qian, X. W. Lin, F. Xu, W. Hu, and Y. Q. Lu, "A three-beam path photonic crystal fiber modal interferometer and its sensing applications," J. Appl. Phys. **108**, 023107 (2010).
7. S. S. Li, Z. D. Huang, X. S. Song, S. Y. Zhang, Q. Zhong, F. Xu, and Y. Q. Lu, "Photonic crystal fibre based high temperature sensor with three-beam path interference," Electron. Lett. **46**, 1394–1396 (2010).
8. R. Jha, J. Villatoro, G. Badenes, and V. Pruneri, "Refractometry based on a photonic crystal fiber interferometer," Opt. Lett. **34**, 617–619 (2009).
9. J. Villatoro, V. P. Minkovich, V. Pruneri, and G. Badenes, "Simple all-microstructured-optical-fiber interferometer built via fusion splicing," Opt. Express **15**, 1491–1496 (2007).
10. V. P. Minkovich, J. Villatoro, D. Monzon-Hernandez, S. Calixto, A. B. Sotsky, and L. I. Sotskaya, "Holey fiber tapers with resonance transmission for high-resolution refractive index sensing," Opt. Express **13**, 7609–7614 (2005).
11. E. J. Zhang, W. D. Sacher, and J. K. S. Poon, "Hydrofluoric acid flow etching of low-loss subwavelength-diameter biconical fiber tapers," Opt. Express **18**, 22593–22598 (2010).
12. G. Brambilla, "Optical fibre nanowires and microwires: a review," J. Opt. **12**, 043001 (2010).

13. G. Brambilla, F. Xu, and X. Feng, "Fabrication of optical fibre nanowires and their optical and mechanical characterisation," Electron. Lett. **42**, 517–519 (2006).
14. G. Brambilla, F. Xu, P. Horak, Y. Jung, F. Koizumi, N. P. Sessions, E. Koukharenko, X. Feng, G. S. Murugan, J. S. Wilkinson, and D. J. Richardson, "Optical fiber nanowires and microwires: fabrication and applications," Adv. Opt. Photon. **1**, 107–161 (2009).
15. T. Wei, Y. K. Han, Y. J. Li, H. L. Tsai, and H. Xiao, "Temperature-insensitive miniaturized fiber inline Fabry-Perot interferometer for highly sensitive refractive index measurement," Opt. Express **16**, 5764–5769 (2008).